Analyzing Effects of Directional Deafness on mmWave Channel Access in Unlicensed Bands

Olga Galinina†, Alexander Pyattaev, Kerstin Johnsson,
Sergey Andreev, and Yevgeni Koucheryavy

***Abstract*—Directional deafness problem is one of the most important challenges in beamforming-based channel access at mmWave frequencies, which is believed to have detrimental effects on system performance in form of excessive delays and significant packet drops. In this paper, we contribute a quantitative analysis of deafness in directional random access systems operating in unlicensed bands by relying on stochastic geometry formulations. We derive a general numerical approach that captures the behavior of deafness probability as well as provide a closed-form solution for a typical sector-shaped antenna model, which may then be extended to a more realistic two-sector pattern. Finally, employing contemporary IEEE 802.11ad modeling numerology, we illustrate our analysis to reveal the importance of deafness-related considerations and their system-level impact.**

I. Research Motivation

A. Introduction

Located at the intersection of human and machine realms, next-generation wearables create a new powerful user interface to the physical world, which may involve people, artificial agents, and robots, as well as massive sensor networks. They also promise to decisively augment our senses and physical abilities. Consequently, it is expected that the market for wearable devices will grow almost four-fold by 2022 [1]. However, high-end wearables, such as augmented and virtual reality (AR/VR) gear, pose unprecedented challenges with their stringent wireless connectivity requirements along the lines of extreme throughput, ultra-low latency, and very high reliability.

The only feasible alternative to enable advanced wearable networks in the emerging 5G-grade use cases (e.g., wireless AR/VR glasses transmitting high-definition video [2]) is the use of extremely high frequency (EHF) bands commonly referred to as *millimeter-wave* (mmWave) [3]. With the impending mass market adoption of high-rate and low-latency wearable applications, mmWave radio technology – with its wider bandwidths, higher achievable data rates, and better frequency reuse capabilities – has the potential to resolve fundamental challenges that cannot be addressed by relying on the legacy short-range radio solutions, such as Bluetooth or WiFi [4].

O. Galinina, S. Andreev, and Y. Koucheryavy are with Laboratory of Electronics and Communications Engineering, Tampere University of Technology, Tampere, Finland.

A. Pyattaev is with YL-Verkot, Tampere, Finland.

K. Johnsson is with Intel Corporation, Santa Clara, CA, USA.

†O. Galinina is the contact author: P.O. Box 553, FI-33101 Tampere, Finland; e-mail: olga.galinina@tut.fi

B. Rationale

Even though relevant research activities on employing mmWave communications technology are already underway, relatively little has been done to design radio access procedures that are explicitly mindful of conditions specific for mmWave. Indeed, while mmWave communications bring along highly-directional physical-layer links, which are different from those in traditional microwave system design, the state-of-the-art wireless standards adopt legacy access control procedures without adapting to the specifics of directional transmissions.

For instance, in unlicensed-band IEEE 802.11ad specifications [5], [6], the distributed coordination function (DCF) is inherited from IEEE 802.11n technology, but now covers the cases where both the transmitter and the receiver operate in directional mode. To date, due to highly limited volumes of IEEE 802.11ad-compatible mmWave products, the potential problems caused by this inefficient approach remain unquantified. However, as increasingly large numbers of such devices are deployed, it will become crucially important to address the aspects of directionality more thoroughly.

In particular, the *deafness problem* is considered to be one of the most important challenges in the beamforming-oriented DCF alternatives. The emergence of the deafness effect is tightly coupled with the contention control mechanism of DCF that can be decomposed into the following phases:

- in the conventional omnidirectional case, the device initiating or accepting a new connection (termed here "primary initiator") announces its intention in every direction (by sending an RTS or CTS message), thus preventing incoming connections to itself;
- in the directional (based on beamforming) case, the primary initiator does not broadcast its RTS in every direction, but rather sends it to its intended target (as it could be interfering with other existing transmissions if not using directional mode);
- similarly, the respondent of the primary initiator (termed here "*primary responder*") replies with a CTS message in the directional mode as well;
- finally, the primary link (between the primary initiator and the respective responder) is established, while a number of other devices proximate to the primary link members may be unaware of this, and are likely to attempt communicating with the primary link members.

The said deafness problem arises when a particular device external to the primary link (termed here "*secondary initiator*") sends an RTS message to the primary link device and

does not receive any response. The secondary initiator then invokes a backoff procedure and might continue attempting to reach its target device repeatedly. Despite no actual contention on the link, the backoff window of the secondary initiator might become inflated, and the data packet might be dropped in the process due to multiple RTS failures. Despite a significant volume of literature on variations of directional CSMA/CA protocols and coordination methods within the context of deafness [7], [8], [9], to the best of our knowledge there has been significantly less attention to quantitative analysis of directional deafness in terms of when and how disruptive for the network the effects of such deafness might be.

In this paper, by relying on stochastic geometry considerations, we target to investigate the above deafness problem, so as to gauge its significance for a wide range of practical mmWave deployments. The rest of this paper is organized as follows. Section II introduces our baseline geometrical model holding the information that is essential for assessing the deafness effects as required for system-level analysis. Section III formulates an expression for the deafness probability in the general case and, in particular, for a widely-adopted sector-shaped mmWave beamforming pattern as well as the more precise two-sector pattern. Finally, we support our analytical findings with numerical results illustrated by means of CSMA/CA protocol operation and access delay assessment in Section IV as well as draw conclusions in Section V.

II. System Model

In order to assess the effects of deafness in directional access, we formulate the minimal feasible system model that is able to characterize the problem at hand. This section provides a description of such model by introducing its core assumptions.

A. Geometry

We consider a tagged mmWave device C that aims at establishing a connection to an already active device A (e.g., an access point) that is selected randomly according to a certain rule. The distances d between C and A may be arbitrary; however, they are assumed to be constrained by the radius of a certain service area R_d (see Fig. 1), where devices desire to establish a connection. Further, we assume that the target device A communicates with its own responder B that is located randomly at the distance of $x \leq R_d$, which follows the distribution $f(x)$. Specifically, as a particular case, we will refer to the uniform distribution of B within the circle of radius R_d around A, and thus the distribution $f(x)$ follows the well-known formulation and equals $\frac{2x}{R_d^2}$. The angle α between the links AB and AC is assumed to be distributed uniformly over the interval $[0, \pi]$.

B. Directivity

All mmWave devices in our network transmit in *directional mode* and receive *omni-directionally*. We further assume that antenna directivity patterns have identical shapes, which are symmetrical with regards to the main beam direction as represented by a function $\rho(\alpha)$ of the relative angle $\alpha \in [0, \pi]$, see e.g., Fig. 2(b). We also normalize the directivity function such that $\rho(0) = 1$, which implies that the total directivity in any direction α is defined by $D_0\rho(\alpha)$, where D_0 is the antenna gain along the main beam symmetry axis. Employing an approximation of the antenna pattern in the form of an elliptical area, we may calculate the maximum directivity as:

$$D_0 = \frac{2}{1 - \cos\frac{\theta}{2}}, \tag{1}$$

where θ is the beam width. The latter corresponds to an idealistic antenna (e.g., as in our special case below), while for other options we recalculate the gain similarly. An example of the practical beamforming pattern is illustrated in Fig. 2(a) [10].

Here, we additionally note that the maximum distance $R, R > R_d$, between a *directional* transmitter and an *omni-directional* receiver corresponds to a certain sensitivity threshold at the minimum received power, and its maximum could be estimated as:

$$R = \sqrt{\frac{P_{tx}\lambda^2 D_0}{(4\pi)^2 N_{thr}}}, \tag{2}$$

where P_{tx} is the transmit power set for all of the devices, λ is the wavelength, N_{thr} is the receiver sensitivity at control PHY, and D_0 is the antenna directivity in case where directional antenna is aligned perfectly.

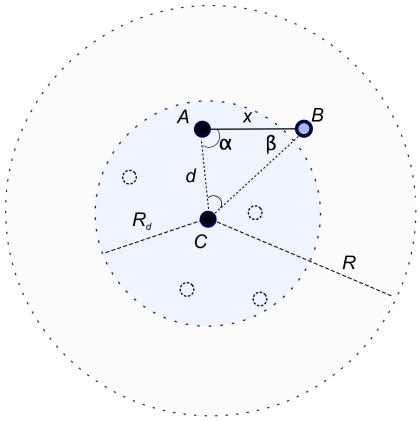

Fig. 1. Illustration of our modeling considerations.

C. Deafness

When the tagged mmWave device C decides to send its request to an already active device A, two outcomes may occur. First, when sensing the channel, it might receive a message (RTS, CTS, or data) from either of the two devices in the requested link. Then, the device C sets its NAV timer and awaits for the primary link AB to expire in the regular mode (outcome I). In the alternative case where no signal is received by the secondary initiator C, it will continue to periodically transmit RTS messages after regular backoff intervals (outcome II). The latter event is referred to as the *deafness problem* and constitutes the key effect of our interest.

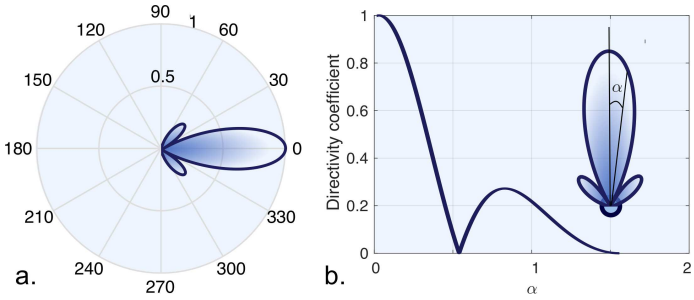

Fig. 2. An example of a beamforming pattern.

III. Deafness Analysis

A. General Case

Here, we derive a general expression for calculating the probability of deafness at the distance of d given a particular distribution of distances $f(x)$ and uniform angles α. The following Theorem summarizes our proposed solution.

Theorem 1. *For a particular distance of d between the tagged mmWave device and its intended respondent, the probability of deafness is given by:*

$$\Pr(\textit{deafness}|d) = \frac{1}{\pi}\int_0^{\pi}\int_0^{R_d} \mathbb{1}\Big[\rho(\alpha) < \tfrac{d^2}{R^2}, \rho(\beta) < \tfrac{d_{BC}^2}{R^2}\Big] f(x) dx d\alpha, \tag{3}$$

where $\mathbb{1}(.)$ is an indicator function, and:

$$d_{BC} = \sqrt{x^2 + d^2 - 2xd\cos\alpha}, \beta = \arccos\left(\tfrac{x - d\cos\alpha}{d_{BC}}\right).$$

Proof. First, let us fix the angle of $\alpha \in [0, \pi)$ between the links AB and AC, as well as the distances x and d, which together determine the shape of the triangle under consideration. Further, we denote the angle $\angle ABC$ as β. Then, for omni-directional reception and directional transmission, the powers at the tagged device C received from the devices A and B are given by:

$$\begin{aligned} P_{rx,A} &= P_{tx} D_0 \rho(\alpha) \tfrac{\lambda^2}{(4\pi)^2 d^2} = C_0 \tfrac{\rho(\alpha)}{d^2}, \\ P_{rx,B} &= P_{tx} D_0 \rho(\beta) \tfrac{\lambda^2}{(4\pi)^2 d_{BC}^2} = C_0 \tfrac{\rho(\beta)}{d_{BC}^2}, \end{aligned} \tag{4}$$

where $C_0 = P_{tx} D_0 \frac{\lambda^2}{(4\pi)^2} = N_{thr} R^2$ is a constant introduced for the sake of brevity and d_{BC} is the distance between the devices B and C. Here, the coefficient $\rho(.)$ scales the directivity according to a deviation from the beam axis. In particular, $\rho(\alpha)$ and $\rho(\beta)$ are defined by the directions of transmission from A and B towards device C.

We note that the receiving device is not capable of differentiating between the signal and noise if $P_{rx,A} < N_{thr}$ ($P_{rx,B} < N_{thr}$). The said device experiences deafness *iff* it is not able to hear both A and B. Therefore, the sought deafness probability is given by:

$$\begin{aligned} \Pr(\text{deafness}|d) = \Pr\left(P_{rx,A} < N_{thr}, P_{rx,C} < N_{thr}|d\right) = \\ \Pr\left(\rho(\alpha) < \tfrac{d^2}{R^2}, \rho(\beta) < \tfrac{d_{BC}^2}{R^2}|d\right) = \\ \frac{1}{\pi}\int_0^{\pi}\int_0^{R_d} \mathbb{1}\Big[\rho(\alpha) < \tfrac{d^2}{R^2}, \rho(\beta) < \tfrac{d_{BC}^2}{R^2}\Big] f_x(x) dx d\alpha, \end{aligned} \tag{5}$$

where $\mathbb{1}(.)$ is an indicator function and:

$$d_{BC} = \sqrt{x^2 + d^2 - 2xd\cos\alpha}, \quad \beta = \arccos\left(\tfrac{x - d\cos\alpha}{d_{BC}}\right),$$

which are obtained from the cosine theorem. □

We note that for (3) one may easily obtain numerical values for the deafness probability with the required precision. However, for some particular cases of the beamforming pattern and the distribution $f(x)$ it is possible to derive closed-form expressions. The following subsections provide derivations of deafness probability for a simpler antenna shape and the uniform distribution of locations of the device B within a circle service area around an access point A.

B. Special Case: Sector

Here, let us consider a typical assumption on the shape of the beamforming pattern: it is represented by a sector of width $\theta \in (0, \pi)$. Consequently, the function $\rho(\alpha)$ is essentially a step function, such that:

$$\rho(\alpha) = \begin{cases} 1, & \text{if } \alpha \le \theta/2, \\ 0, & \text{otherwise.} \end{cases} \tag{6}$$

With respect to the shape of $\rho(\alpha)$, we focus on the expression under the integral sign (3):

$$\mathbb{1}\Big[\rho(\alpha) < \tfrac{d^2}{R^2}, \rho(\beta) < \tfrac{d_{BC}^2}{R^2}\Big]. \tag{7}$$

Hereinafter, we assume for simplicity that the service area $R_d < 0.5R$; hence, the distance d_{BC} cannot exceed the maximum threshold distance R. Importantly, if otherwise $R_d > 0.5R$, then the following calculation may easily be extended by an additional integral expression. However, for realistic settings and beam widths $R_d < 0.5R$ holds, and the additional integral always vanishes. Based on this assumption and the *uniform distribution* of device B within a circle around A, we formulate the following Theorem.

Theorem 2. *For the distribution of distances $f(x) = \frac{2x}{R_d^2}$, where the service area has the radius of $R_d < 0.5R$, the probability of deafness may be found as:*

$$\Pr\{\textit{deafness}|d < P_d \sin\tfrac{\theta}{2}\} = \tfrac{d^2}{\pi R_d^2}\left[\tfrac{\pi - \theta + \sin\theta\cos\theta}{1 - \cos\theta}\right], \tag{8}$$

and

$$\begin{aligned} \Pr\{\textit{deafness}|d \ge P_d \sin\tfrac{\theta}{2}\} = \Pr\{\textit{deafness}|d < P_d \sin\tfrac{\theta}{2}\} - \\ \tfrac{d^2}{\pi R_d^2}\left[\tfrac{2(\tilde{z}_2 - \tilde{z}_1) + \sin(2\tilde{z}_1 + \theta) - \sin(2\tilde{z}_2 + \theta)}{2(1 - \cos\theta)}\right], \end{aligned} \tag{9}$$

where $\tilde{z}_1 = \max\{\frac{\theta}{2}, z_1\}$, $\tilde{z}_2 = \min\{\pi - \frac{\theta}{2}, z_2\}$, and $z_{1,2}$ are given by:

$$z_{1,2} = \tfrac{P_d}{d}\sin^2\tfrac{\theta}{2} \pm \cos\tfrac{\theta}{2}\sqrt{1 - \left(\tfrac{P_d}{d}\right)^2 \sin^2\tfrac{\theta}{2}}.$$

Proof. Given the expression under the integral (3) and the fact that $\cos\beta = \frac{x - d\cos\alpha}{d_{BC}}$, we may rewrite the sought probability as:

$$\begin{aligned} \Pr\left(\text{deafness}\right) = \Pr\left(\rho(\alpha) < \tfrac{d^2}{R^2}, \rho(\beta) < \tfrac{d_{BC}^2}{R^2}\right) = \\ \Pr\left(\alpha > \tfrac{\theta}{2}, \beta > \tfrac{\theta}{2}\right) = \Pr\left(\alpha > \tfrac{\theta}{2}, \tfrac{x - d\cos\alpha}{d_{BC}} < \cos\tfrac{\theta}{2}\right). \end{aligned} \tag{10}$$

Expanding d_{BC} and recombining the second condition in (10), we obtain an equivalent:

$$(x - d\cos\alpha) < d\cot\tfrac{\theta}{2}\sin\alpha, \tag{11}$$

for $x - d\cos\alpha > 0$, while for $x - d\cos\alpha \le 0$ the second condition always holds. Consequently, for the CDF $F(x) = \frac{x^2}{R_d^2}$ and $\cos\alpha + \sin\alpha\cot\frac{\theta}{2} > 0$ (which is equivalent to $\alpha < \pi - \frac{\theta}{2}$), we may rewrite the sought probability as:

$$\begin{aligned}\Pr(\text{deafness}) = \Pr\big(\alpha > \tfrac{\theta}{2}, x < d\big(\cos\alpha + \sin\alpha\cot\tfrac{\theta}{2}\big)\big) + \\ \Pr\big(\tfrac{\theta}{2} < \alpha < \pi - \tfrac{\theta}{2}, 0 < x < d\big(\cos\alpha + \sin\alpha\cot\tfrac{\theta}{2}\big)\big).\end{aligned} \tag{12}$$

We note that the expression $d\left(\cos\alpha + \sin\alpha\cot\frac{\theta}{2}\right)$ may exceed the maximum value R_d for x. Therefore, assuming $z(\alpha) = \left(\cos\alpha + \sin\alpha\cot\frac{\theta}{2}\right)$, we split the above into two parts:

$$\begin{aligned}\Pr(\text{deafness}) = \Pr\big(\tfrac{\theta}{2} < \alpha < \pi - \tfrac{\theta}{2}, z(\alpha) \ge \tfrac{R_d}{d}\big) + \\ \Pr\big(\tfrac{\theta}{2} < \alpha < \pi - \tfrac{\theta}{2}, x < d\cdot z(\alpha), z(\alpha) < \tfrac{R_d}{d}\big).\end{aligned} \tag{13}$$

In order to solve the inequality $z(\alpha) < \frac{R_d}{d}$, we consider the equation $\sin\alpha\cot\frac{\theta}{2} = \frac{R_d}{d} - \cos\alpha$, which results in the following roots since its both parts are positive:

$$z_{1,2} = \tfrac{P_d}{d}\sin^2\tfrac{\theta}{2} \pm \cos\tfrac{\theta}{2}\sqrt{1 - \left(\tfrac{P_d}{d}\right)^2\sin^2\tfrac{\theta}{2}}. \tag{14}$$

Here, Fig. 3 illustrates the behavior of the function $z(\alpha)$ over the interval $[0, \pi]$ of the parameter α with the maximum at the point $\left(\frac{\pi}{2} - \frac{\theta}{2}, \frac{1}{\sin\frac{\theta}{2}}\right)$, which can be established easily. Importantly, in case when $d < P_d\sin\frac{\theta}{2}$, the line is located above the curve and no real roots exist. This leads us to the conclusion that for $d > P_d\sin\frac{\theta}{2}$, $z(\alpha)$ exceeds the threshold $\frac{R_d}{d}$ if $\alpha \in (\max\{\frac{\theta}{2}, z_1\}, \min\{\pi - \frac{\theta}{2}, z_2\})$ and therefore:

$$\begin{aligned}\Pr\big(\tfrac{\theta}{2} < \alpha < \pi - \tfrac{\theta}{2}, z(\alpha) \ge \tfrac{R_d}{d}\big) = \\ \tfrac{1}{\pi}\left(\min\left\{\pi - \tfrac{\theta}{2}, z_2\right\} - \max\left\{\tfrac{\theta}{2}, z_1\right\}\right) = \tfrac{1}{\pi}\left(\tilde{z}_2 - \tilde{z}_1\right),\end{aligned}$$

where $\tilde{z}_1 = \max\{\frac{\theta}{2}, z_1\}$ and $\tilde{z}_2 = \min\{\pi - \frac{\theta}{2}, z_2\}$. For the other values of α, the limiting expression for x (i.e., $d\cdot z(\alpha) < R_d$) can thus be taken into account together with the distribution $f_x(x)$. Hence, the expression for the second component of (13) may be rewritten as:

$$\begin{aligned}\Pr\big(\tfrac{\theta}{2} < \alpha < \pi - \tfrac{\theta}{2}, x < d\cdot z(\alpha), z(\alpha) < \tfrac{R_d}{d}\big) = \\ \frac{d^2}{\pi R_d^2}\left[\int_{\frac{\theta}{2}}^{\tilde{z}_1}\left(\cos\alpha + \sin\alpha\cot\tfrac{\theta}{2}\right)^2 d\alpha + \int_{\tilde{z}_2}^{\pi - \frac{\theta}{2}}\left(\cos\alpha + \sin\alpha\cot\tfrac{\theta}{2}\right)^2 d\alpha\right] = \\ \frac{d^2}{\pi R_d^2}\left[\frac{2\theta - 2\pi + 2(\tilde{z}_2 - \tilde{z}_1) + \sin(2\tilde{z}_1 + \theta) - \sin(2\tilde{z}_2 + \theta) - \sin(2\theta)}{2(\cos\theta - 1)}\right].\end{aligned} \tag{15}$$

Finally, we establish for $d \ge \frac{P_d}{d}\sin\frac{\theta}{2}$:

$$\begin{aligned}\Pr\{\text{deafness} | d \ge P_d\sin\tfrac{\theta}{2}\} = \tfrac{1}{\pi}\left(\tilde{z}_2 - \tilde{z}_1\right) + \\ \frac{d^2}{\pi R_d^2}\left[\frac{\pi - \theta + \sin\theta\cos\theta}{1 - \cos\theta} - \frac{2(\tilde{z}_2 - \tilde{z}_1) + \sin(2\tilde{z}_1 + \theta) - \sin(2\tilde{z}_2 + \theta)}{2(1 - \cos\theta)}\right],\end{aligned} \tag{16}$$

while for $d < P_d\sin\frac{\theta}{2}$ a simpler expression holds:

$$\begin{aligned}\Pr\{\text{deafness} | d < P_d\sin\tfrac{\theta}{2}\} = \\ \frac{d^2}{\pi R_d^2}\int_{\frac{\theta}{2}}^{\pi - \frac{\theta}{2}}\left(\cos\alpha + \sin\alpha\cot\tfrac{\theta}{2}\right)^2 d\alpha = \frac{d^2}{\pi R_d^2}\left[\frac{\pi - \theta + \sin\theta\cos\theta}{1 - \cos\theta}\right].\end{aligned} \tag{17}$$

□

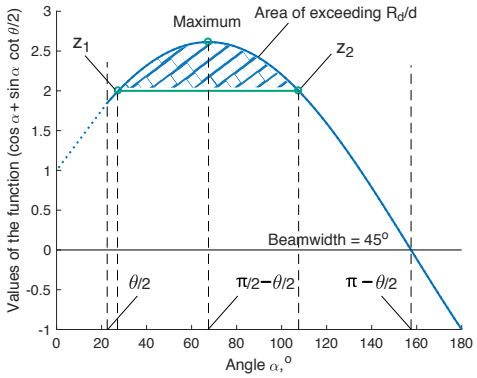

Fig. 3. Illustration of the proof of Theorem 2 for $R_d = 40, d = 20, \theta = \frac{\pi}{4}$: values of $z(\alpha) = \left(\cos\alpha + \sin\alpha\cot\frac{\theta}{2}\right)$ (blue curve), roots z_1, z_2, and the point of maximum (markers). The line segment between z_1, z_2 corresponds to the ratio $\frac{P_d}{d}$, while the upper part (highlighted area) defines the interval where $z(\alpha) \ge \frac{P_d}{d}$.

Below we provide an extension of the considered sector model, which may serve as a better approximation for the realistic beamforming pattern as shown in Section IV.

C. Special Case: Two Sectors

We note that the above approximation by the sector antenna is relatively coarse, primarily due to the fact that it disregards the presence of sidelobes. One possible way to extend this approximation could be to consider an antenna with the beamforming pattern represented by a sector and a circle of a smaller radius r_0. However, when evaluating deafness effects, such a model would not permit for the analysis at shorter distances by yielding strictly zero deafness probability i.e., when $d \le \sqrt{r_0}R$ that for the narrower beams may cover the entire interval $(0, R_d)$.

As an alternative able to incorporate the antenna sidelobes but yet remain analytically tractable, we propose the following two-sector model for the beam width $\theta < \pi$:

$$\rho(\alpha) = \begin{cases} 1, & \text{if } \alpha \le \theta/4, \\ r_0, & \text{if } \theta/4 \le \alpha \le \theta/2, \\ 0, & \text{otherwise.} \end{cases} \tag{18}$$

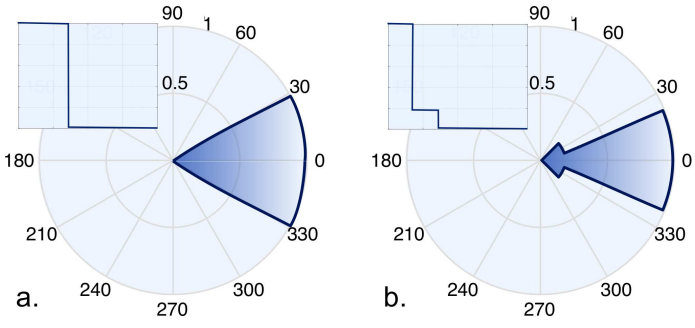

Fig. 4. Illustration of tractable antenna models: (a) sector, (b) two-sector beamforming patterns.

Here, the width of the narrower beam may be as well selected differently, whilst $\theta/4$ is taken by analogy with FFT antenna pattern generation. The parameter r_0 may be chosen

based on the ratio between the mainlobe and the sidelobes powers. The directivity gain should also be recalculated similarly to (1):

$$D'_0 = \frac{2}{1-\cos\frac{\theta}{4}+r_0(\cos\frac{\theta}{4}-\cos\frac{\theta}{2})}. \quad (19)$$

Further, we return to the expression under the integral sign (3) and revisit the deafness definition assuming $R_d < 0.5R$:

$$\text{Deafness} = \left\langle \rho(\alpha) < \frac{d^2}{R^2}, \rho(\beta) < \frac{d_{BC}^2}{R^2} \right\rangle = \begin{cases} \left\langle \alpha > \frac{\theta}{2}, \quad \beta > \frac{\theta}{2} \right\rangle, \text{ or} \\ \left\langle \alpha > \frac{\theta}{2}, \quad \frac{\theta}{4} < \beta \le \frac{\theta}{2}, \quad d_{BC} > \sqrt{r_0}R \right\rangle, \\ \left\langle \frac{\theta}{4} < \alpha \le \frac{\theta}{2}, \quad d > \sqrt{r_0}R, \quad \beta > \frac{\theta}{2} \right\rangle, \\ \left\langle \frac{\theta}{4} < \alpha \le \frac{\theta}{2}, \quad d > \sqrt{r_0}R, \quad \frac{\theta}{4} < \beta \le \frac{\theta}{2}, \quad d_{BC} > \sqrt{r_0}R \right\rangle. \end{cases} \quad (20)$$

We note that the probability of the first event is given by Theorem 1 for the maximum distance R', as should be recalculated for the renewed directivity gain according to (2). Derivation of the probabilities of the following three events is relatively simple (although bulky) and constitutes a technical exercise, which we omit here due to the space constraints.

IV. Numerical Results

In this section, we illustrate the above discussion as well as interpret the probability of deafness in terms of the resulting MAC performance by modeling a realistic network scenario in our WinterSim framework[1].

A. Deafness Probability

Here, we compare the deafness probability for an arbitrary antenna (3) and the simplified sector-shaped beamforming patterns that are analytically tractable in most of the stochastic geometry models. In particular, we refer to uniform rectangular 2x2, 4x4, 8x8, and 16x16 arrays of cosine antenna elements, as well as construct the antenna analyzer in MATLAB (see Fig. 5).

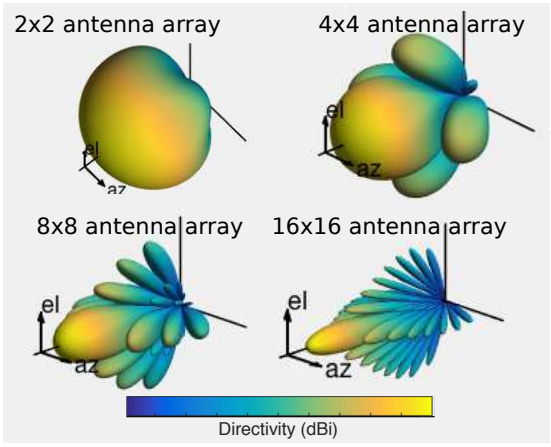

Fig. 5. 3D beamforming pattern for 2x2, 4x4, 8x8, and 16x16 rectangular antenna arrays.

The dependence of the deafness probability on the distance between the tagged device C and the access point A is illustrated in Fig. 6, where we collect not only results for the above realistic antenna settings but also for the sector-shaped antennas. Clearly, we may observe that despite the variations in the antenna properties (see Chebyshev and Hamming taper), the shape of the curves remains relatively constant for selected settings. Even though the sector antenna repeats the same trend as the realistic ones, from the quantitative point of view the divergence is rather visible.

In Fig. 7(a) and (b), we provide a dense set of curves built for the sector and two-sector antenna, respectively. We note that although the sector-shaped antenna follows the same law as the realistic antennas, for the wider beams it becomes difficult to select an appropriate approximation. In contrast, for the narrow beams one may find a suitable option which, however, has to be adjusted accordingly (i.e., typical values of beam width may result in extremely high divergence as in Fig. 7). In turn, two-sector antennas become a more precise approximation for all the ranges of the beam width.

Moreover, we may observe that deafness becomes a significant problem for any beamforming system once the initiator becomes sufficiently far away from the access point, and as such may cause considerable disruptions to the network operation.

TABLE I
Numerical Modeling Parameters

Parameter	Value
Carrier	60 GHz
Spatial streams	1 (SISO)
Sensitivity	−78 dBm
Transmit power	23 dBm
Beam width	22.5, 45, and 90 degrees
Radius of service area R_d	40 m
Number of devices N	10
TXOP duration	1.3 ms
Maximum queue length	50 AMPDUs
CW_{min}	8 slots
CW_{max}	1024 slots
Retry limit R_{max}	7 retries

B. Simulation Settings

In our further simulation-based study, we evaluate the impact of deafness on 802.11ad MAC procedures. Specifically, we base our approach on modeling of the DCF access scheme with RTS/CTS handshake in a contention-based access mode, as specified in the IEEE 802.11ad-2012 standard. The association procedures, beamforming training and tracking, and beaconing functions are omitted here for simplicity.

Further, we assume N devices (STAs) associated with an access point (AP), so that any of them may occupy the shared channel for exactly one transmission opportunity (TXOP) every time it acquires access to the channel. Each device is allowed to transmit exactly one aggregated packet (AMPDU) during that time. The deafness is defined as an event when RTS has been sent to the AP, which at the moment has its NAV set (i.e., is currently serving another STA).

We refer to the total system load as to $\frac{\kappa}{N}$ AMPDUs per TXOP at each STA, while every STA adheres to a Bernoulli arrival process. All STAs are initialized with empty queues and only uplink (STA-initiated) transmissions are considered. The

[1] http://winter-group.net/downloads/

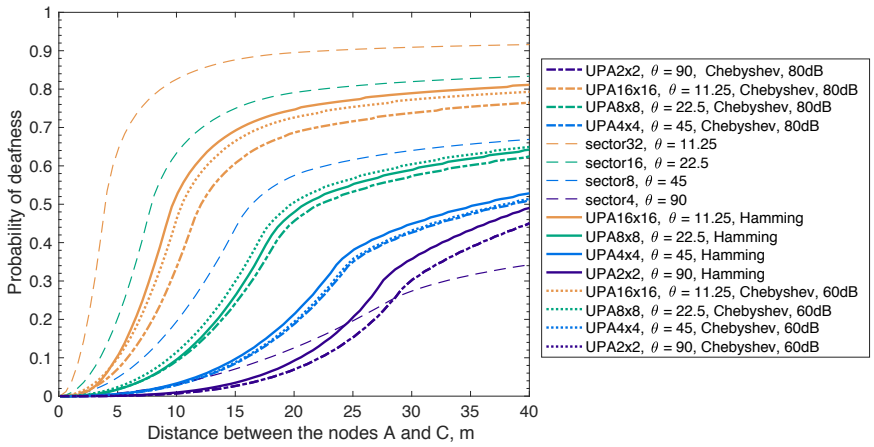

Fig. 6. Probability of deafness vs. distance between A and C.

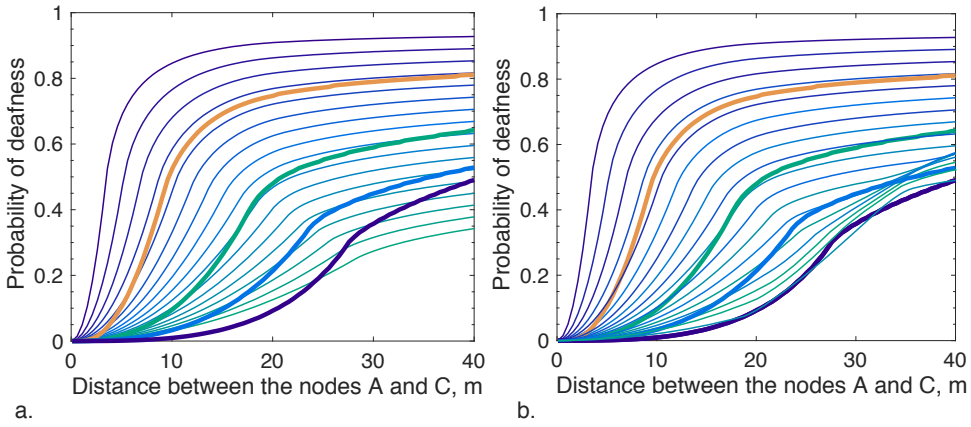

Fig. 7. Illustration of realistic 2x2, 4x4, 8x8, and 16x16 antenna approximations: (a) by sector beamforming pattern and (b) by two-sector antenna pattern. The baseline curves for comparison are highlighted in bold and maintain the same color scheme as in Fig. 6.

system load of 1 thus corresponds to the maximum theoretical system capacity, if no overheads are present, and beyond this point the system is highly unstable. The core simulation parameters are presented in Table I.

C. Protocol Impact Study

While our simulation scenario is relatively straightforward, the impact of deafness on the DCF protocol is, however, much more complex and ambiguous. Most effects of deafness prove to be strictly negative:

- deafness causes multiple consecutive CTS timeouts;
- CTS timeouts yield contention window (CW) growth;
- CW growth leads to excessive delays and even packet drops.

On the other hand, some side-effects of deafness may be seen as "beneficial" for the system performance:

- STAs that experience deafness issues do not participate in contention (due to their large CWs);
- the average CW on other STAs and thus the backoff delay are reduced;
- the throughput of the system may improve, while the multiplexing delay is reduced (as the effective number of participants N decreases).

To capture the above system dynamics, we track both the packet losses that are due to timeouts and the queue overflows, as well as provide statistics on the time spent in serving both successfully delivered and dropped packets. This allows us to observe all of the above mentioned system effects.

To quantify the delay induced by deafness, let us first examine the average amount of time spent while serving a packet (see Fig. 8). The time interval of interest starts at the arrival into the transmitter queue (i.e., includes queuing and actual MAC procedures) and ends with the packet either being acknowledged by the AP or dropped at the source STA, with both cases shown in the figure.

One may clearly observe that with the beam width reduced, the expected delay rises sharply by reaching over $10\,\mathrm{ms}$ under the load of $70\,\%$. We note that the multiplexing delay is also included here, but its contribution constitutes only $4\,\mathrm{ms}$ at the same load level (as shown by the black curve).

Importantly, the maximum delay does not correspond to the highest deafness probability. Indeed, when the deafness is

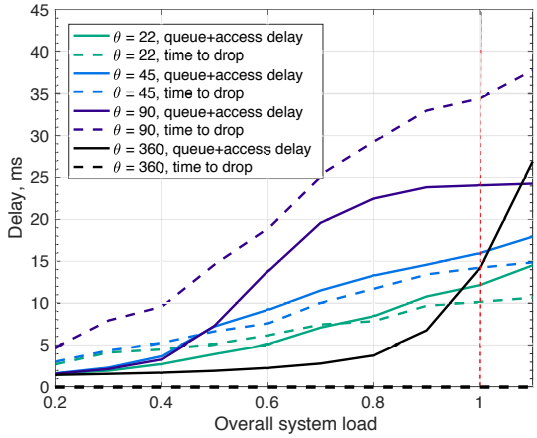

Fig. 8. Average service delay and time before dropping vs. system load κ.

nearly $100\,\%$, the packets are dropped faster, thus allowing the STAs to initiate new transmissions. However, at 90° we observe the worst case: deafness does impact the system, but not sufficiently to cause packet loss and CW reset; consequently, channel access becomes delayed instead. As a result, time to drop exceeds $30\,\mathrm{ms}$ in some cases, so that the system becomes unusable for most of the typical mmWave applications.

Further, let us investigate the packet loss rates demonstrated in Fig. 9. Clearly, the highest drop rates correspond to the maximum deafness probability, as expected. The plot distinctly shows that for 90° beam width almost no packets are dropped, and that in turn causes excessive delays, as explained previously.

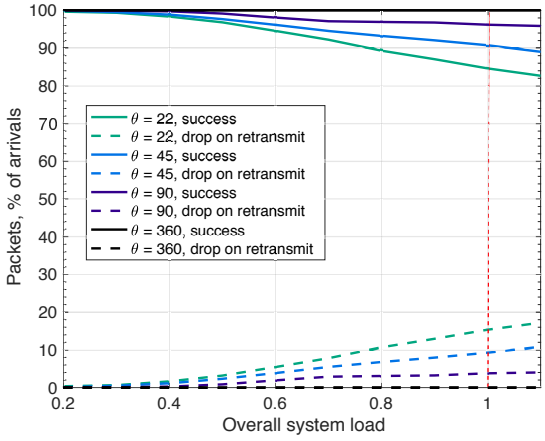

Fig. 9. Average drop rate vs. system load κ.

While the observed drop rates might appear relatively moderate for a practical wireless system, note that they occur after 8 failed transmissions, and as such should be corrected by the upper layers. Most importantly, for a transport protocol such as TCP, for instance, a packet loss rate of $10\,\%$ might cause close to a complete stall of data transfer, while real-time video and voice communications quality might drop to unacceptably low levels.

Based on the obtained results, we conclude that due to the packet losses and excessive delays the observed WLAN system prone to deafness effects can only serve users satisfactorily under the loads of below $40\,\%$.

V. Conclusions

In this paper, we have contributed the following:

- a sector-shaped stochastic geometry model to calculate the probability of deafness in typical directional mmWave connectivity scenarios together with more precise two-sector antenna modeling; both formulations incorporate important input parameters and remain analytically tractable;
- numerical results that confirm the applicability of both proposed models in relation to realistic antenna patterns;
- practical assessment and numerical evaluation of the impact that deafness has on the channel access in unlicensed-band mmWave systems, including IEEE 802.11ad and beyond (such as the emerging IEEE 802.11ay specifications).

In summary, we believe that directional deafness has a detrimental impact on the MAC-layer performance, thus resulting in uncontrolled access delay fluctuations, unpredictable packet loss, and other adverse effects. Based on our results, MAC algorithm developers can be aware of the extent of harm that deafness has, and act accordingly.

Acknowledgment

This work is supported by Intel Corporation as well as by the WiFiUS project funded by the Academy of Finland. The work of O. Galinina is supported in part with a personal research grant by the Finnish Cultural Foundation and in part by a Jorma Ollila grant from Nokia Foundation.

References

[1] Tractica Report, "Wearable Device Market Forecasts," 3Q 2017.
[2] N. Hunn, "The Market for Smart Wearable Technology: A Consumer Centric Approach," 2015.
[3] F. Boccardi, R. W. H. Jr., A. E. Lozano, T. L. Marzetta, and P. Popovski, "Five disruptive technology directions for 5G," *IEEE Communications Magazine*, vol. 52, no. 2, pp. 74–80, 2014.
[4] A. Pyattaev, K. Johnsson, S. Andreev, and Y. Koucheryavy, "Communication challenges in high-density deployments of wearable wireless devices," *IEEE Wireless Communications*, vol. 22, no. 1, pp. 12–18, 2015.
[5] IEEE 802.11 WG, "IEEE 802.11ad, Amendment 3: Enhancements for Very High Throughput in the 60 GHz Band," Dec 2012.
[6] T. Nitsche, C. Cordeiro, A. B. Flores, E. W. Knightly, E. Perahia, and J. Widmer, "IEEE 802.11ad: directional 60 GHz communication for multi-Gigabit-per-second Wi-Fi," *IEEE Communications Magazine*, vol. 52, no. 12, pp. 132–141, 2014.
[7] E. Shihab, L. Cai, and J. Pan, "A Distributed Asynchronous Directional-to-Directional MAC Protocol for Wireless Ad Hoc Networks," *IEEE Transactions on Vehicular Technology*, vol. 58, pp. 5124–5134, Nov 2009.
[8] M. X. Gong, R. Stacey, D. Akhmetov, and S. Mao, "A Directional CSMA/CA Protocol for mmWave Wireless PANs," in *2010 IEEE Wireless Communication and Networking Conference*, pp. 1–6, April 2010.
[9] S. Singh, R. Mudumbai, and U. Madhow, "Distributed Coordination with Deaf Neighbors: Efficient Medium Access for 60 GHz Mesh Networks," in *2010 Proceedings IEEE INFOCOM*, pp. 1–9, March 2010.
[10] D. Tse and P. Viswanath, *Fundamentals of Wireless Communication*. New York, NY, USA: Cambridge University Press, 2005.